SPECIAL FEATURE: PERSPECTIVE

Supercooled and glassy water: Metastable liquid(s), amorphous solid(s), and a no-man's land

Philip H. Handle[a,b,1,2], Thomas Loerting[b,1,2], and Francesco Sciortino[a,1,2]

Edited by Pablo G. Debenedetti, Princeton University, Princeton, NJ, and approved October 3, 2017 (received for review September 1, 2017)

We review the recent research on supercooled and glassy water, focusing on the possible origins of its complex behavior. We stress the central role played by the strong directionality of the water–water interaction and by the competition between local energy, local entropy, and local density. In this context we discuss the phenomenon of polyamorphism (i.e., the existence of more than one disordered solid state), emphasizing both the role of the preparation protocols and the transformation between the different disordered ices. Finally, we present the ongoing debate on the possibility of linking polyamorphism with a liquid–liquid transition that could take place in the no-man's land, the temperature–pressure window in which homogeneous nucleation prevents the investigation of water in its metastable liquid form.

water | amorphous ice | supercooled liquids | liquid–liquid transition | no-man's land

Water, the molecule of life, is literally everywhere. It covers the Earth's surface in the form of lakes, rivers, oceans, ice caps, and glaciers. It fills vast underground caverns and it resides in our atmosphere as vapor or in clouds. However, water is not restricted to Earth. It is found on the planets of our solar system and their moons and on asteroids and comets (1), possibly in its glass (i.e., amorphous ice) form (2). Water as an amorphous solid is also abundant in the interstellar medium (3), where it may play a fundamental role in the formation of complex organic molecules such as amino acids and sugars (4). In light of this ubiquity, it is not surprising that the scientific literature concerned with water and water solutions is immense.

In this paper we focus explicitly on bulk water in metastable conditions, that is, water below its equilibrium melting temperature, both as a supercooled liquid and as an amorphous solid. We attempt to provide insights on the unconventional behavior of water in its liquid and glass form. Indeed, despite water being the most abundant liquid, paradoxically it is scientifically considered anomalous due to its rather complex behavior. For instance, the isobaric heat capacity C_P, the isothermal compressibility K_T, and the viscosity η all show a nonmonotonic temperature T and/or pressure P dependence, which is amplified upon supercooling. The incomplete understanding of the origin of the numerous anomalies motivates the scientific interest in liquid water and even more in its metastable liquid state. Similarly, the disordered solid form of water also has its peculiarities. It displays polyamorphism (amorphous polymorphism), a term created in analogy to crystal polymorphism, indicating the existence of more than one disordered amorphous form.

Since several high-quality reviews focusing on supercooled and glass water have appeared in recent years (5–14), rather than being comprehensive we focus on a limited number of experimental and theoretical investigations. Specifically, we attempt to elucidate the present understanding of bulk (as opposed to confined) water in the supercooled liquid state above the homogeneous nucleation temperature T_h and in the amorphous state below T_x, the temperature at which the glass crystallizes on heating. These two temperatures define the intermediate window in the T–P plane in which only crystalline ice is observed. This window, which present-day research attempts to shrink by working on smaller and smaller samples and better and better aged glasses, is conventionally called no-man's land (15). We also discuss in detail the phenomenon of polyamorphism unraveled by Mishima et al. (16, 17) and Mishima (18) which has been subject to intense debate ever since. Foremost, we aim at briefly mentioning the key findings and pointing to the open questions that split the field, hopefully providing a representation of some of the different ideas proposed to interpret the available experimental results and the associated theoretical frameworks. It is indeed fair to state that even today there is no consensus about the origin of the anomalous

[a]Department of Physics, Sapienza University of Rome, I-00185 Roma, Italy; and [b]Institute of Physical Chemistry, University of Innsbruck, A-6020 Innsbruck, Austria

Author contributions: P.H.H., T.L., and F.S. wrote the paper.

The authors declare no conflict of interest.

This article is a PNAS Direct Submission.

[1]P.H.H., T.L., and F.S. contributed equally to this work.

[2]To whom correspondence may be addressed. Email: philip.handle@uibk.ac.at, thomas.loerting@uibk.ac.at, or francesco.sciortino@uniroma1.it.

behavior of liquid water and about the origin and existence of thermodynamically distinct disordered polyamorphs.

Liquid Water

The Physics of Water. What makes water special compared with other liquids is the strong directional character of the intermolecular interaction potential. The dominant contribution, called the hydrogen bond (HB), has a strength intermediate between the stronger covalent bond and the weaker dipole-induced interaction. In addition, the HB strength is significantly larger than the thermal energy at room T. An HB requires a hydrogen atom pointing toward a close-by oxygen atom. The strength of the HB is maximized when the hydrogen atom is collinear with the acceptor and donor oxygen and progressively weakens on increasing the HOO angle.

The strength of the HB and its directionality are key elements in controlling liquid water's thermodynamic and dynamic behavior. If the HB interaction did not exist, water would behave just like all other H_2X triatomic molecules, with X representing any chalcogen, and it would be gaseous at room T (19). If the interaction between water molecules was isotropic and described by an attraction comparable to the HB strength, the gas–liquid critical T would be located at about one order of magnitude higher temperature than the real experimental value (647 K). What makes water a liquid at ambient T is the directionality of the HBs and the limited number of linear HBs that a molecule can form (at most four). Such limited valence significantly lowers the critical T compared with the isotropic case (20). This originates a liquid phase at room T in which the number of nearest neighbors is around four, significantly lower than the typical value observed in simple liquids, namely 12. Since on cooling percolation precedes the gas–liquid critical point (CP), the liquid phase can be described as a percolating network of HBs (21), constantly restructuring itself on a picosecond time scale.

The directionality of the interaction is responsible for the peculiar correlation between local energy, density, and entropy. The establishment of four linear HBs (a state of low energy) is possible only for well-defined orientations of the water molecule (low entropy and density). The formation of such a state is driven by the decrease in energy but it is contrasted by the decrease in entropy and the increase in the mechanical work (PV, V being volume) term. Similarly, the formation of locally denser arrangements, associated with the presence of additional molecules in the first coordination shell, generates distorted HBs and states with higher local energy and entropy. The formation of these more dense local environments is driven by entropy and PV and contrasted by the energy loss. Both of these structural motifs are found in liquid water. The most prominent examples are environments characterized by four and three linear HBs. In the first case the local arrangement is to a good approximation tetrahedral, while in the second case a fifth neighbor, locally distorting the HB pattern, is present in the first coordination shell (22).

Water's Anomalies. The competition between different local environments has been identified as the source of the anomalies of liquid water, both in its stable and metastable states (21). While in a simple liquid the role of T and P is limited to a smooth change in local properties, in water a change in these control variables modifies the equilibrium between the different local environments. Generically, decreasing T favors fully bonded local configurations, and increasing P favors more distorted ones. Such equilibrium between different classes, which is not found in simple liquids, is responsible for the existence of a T at which the density reaches a maximum value at constant pressure T_{MD} (5). When $T = T_{MD}$ the increase in V associated with the formation of more bonded local configurations compensates the decrease in V associated to the reduction of the thermal vibrations. The latter is the mechanism responsible for contraction on cooling in all materials. Equilibrium between different local environments also explains other anomalies, such as the speeding up of the dynamics on increasing P (molecules with distorted bonds have a larger mobility).

The picture of water as composed of two or more classes of locally structurally distinct molecules is a recurrent theme in water science research, often contrasted with an alternative picture based on a continuum of geometric arrangements. Already the first computer simulations of water (28) provided evidence that all local properties are characterized by broad unimodal distributions with a T and P dependence of the average values, apparently ruling out the possibility of a meaningful definition of distinct local environments. Only recently, progress in data analysis made it possible to show that classes of structurally different local environments can robustly be defined if appropriate order parameters are evaluated (29, 30). These new analyses, applied to novel and old simulation data, show that water molecules differing in their local environment can be treated as species in chemical equilibrium. Interestingly, the ability to resolve these classes requires information on the degree on translational order of the second-nearest-neighbor shell (31), sophisticated Markov state models (32), and, in some cases, the suppression (33) of the vibrational (translational and librational) component via the inherent structure methodology (34).

Are molecules with tetrahedral local order progressively clustering in space on cooling? Does this clustering—which could originate from the highly directional interactions (geometric correlation) and from the redistribution of the electronic density on bonding (polarizable and quantum effects)—become so intense as to induce a complete separation of these differently bonded molecules and possibly distinct disordered liquid phases? The answer to these questions is central in present-day research.

Supercooled Water. Answering the above questions is even more relevant in the description of supercooled water, that is, water below its melting temperature T_m. In this region, where liquid water becomes thermodynamically less stable than ice, it is still possible to perform measurements in the liquid state for times significantly longer than its equilibration time but still shorter than the crystallization time. Eventually, however, nucleation of ice prevails. For our purposes we can simply state that the homogeneous nucleation temperature T_h sets the lower limit of existence of the metastable liquid phase. The T–P region in which nucleation prevents the observation of metastable liquid states has been named "no-man's land" (15). The border to the no-man's land is ill-defined, since the location of T_h depends on the experimental time and on the sample size. Recent experiments (35) show that metastable liquid water can transiently exist on the millisecond time scale down to $T = 227$ K, setting the present upper limit of the no-man's land. The very same study also indicates that tetrahedral ordering increases in supercooled water. At timescales shorter than microseconds crystallization can even be avoided entirely (see *Preparation Routes*).

Possible Explanations. The extrapolation of the thermodynamic response functions into the no-man's land is at the heart of possible thermodynamic scenarios proposed to interpret water's anomalies. The steep rise of K_T and C_P (36, 37) on cooling (after the subtraction of a significant normal component) has been linked to a possible power-law divergence around $T \approx 228$ K and interpreted as originating from a thermodynamic instability.

An elegant explanation of such divergence has been proposed by Speedy (38). In standard liquids, as predicted by the van der Waals theory, the gas–liquid spinodal (the line emanating from the gas–liquid CP defining the mean-field limit of stability of the liquid phase) is monotonic in the P–T plane approaching $T = 0$ K at the maximum tensile ($P < 0$) strength value (39). Speedy (38), however, showed that

thermodynamic constraints impose a reentrant behavior on the spinodal in the P–T plane if the liquid has a T_{MD} line intersecting the spinodal line. If the spinodal traces back to positive P, the liquid becomes unstable to gas-like fluctuations both on heating and on cooling (40). Despite the difficulty of imagining a liquid that would vaporize on cooling, Speedy's scenario is thermodynamically consistent and it has been recently observed in one-component models of patchy colloids (24, 25). In these models the reentrance is provided by closed-loop phase diagrams (Fig. 1 *C* and *D*), where the spinodal starts in the upper CP and terminates at the lower one. According to Debenedetti (5), Speedy's scenario should not be considered as a possible explanation of water's anomalies since there is no experimental evidence of a reentrance of the metastable gas–liquid coexistence line (binodal).

Another possibility is to assume no divergence of the extrapolations of K_T and C_P into the no-man's land but rather a maximum. Such a scenario is often called singularity-free scenario (Fig. 1 *A* and *B*). This scenario is consistent with intuition (and experimental and numerical observations) that supercooled water approaches the structure of a fully bonded random tetrahedral network on cooling. The cross-over from a weakly tetrahedral structure at ambient T to a fully developed tetrahedral structure at very low T suggests indeed a sigmoidal T dependence of the local properties (e.g., energy and volume) and a maximum in their T derivatives. A maximum in the specific heat is typical of systems with quantized energy levels (Schottky anomaly) and commonly observed when particles form a limited number of strong bonds, such that the energy provides a proxy to the number of bonded pairs.

The Ts at which the response functions assume the maximum value, when evaluated at different pressures, define loci in the P–T plane along which fluctuations are maximized. In the LLCP scenario (26, 41) it is assumed that lines of C_P and K_T extrema converge to a common line [Widom line (42)] that emanates from a CP at positive pressures. This novel CP is commonly indicated as the second CP, the gas–liquid CP being the first. This scenario (Fig. 1 *E* and *F*), discovered in computer simulations of the ST2 water model (26, 41), implies that indeed a spatial correlation exists between molecules in tetrahedral and in distorted local environments, resulting in a segregation of the two classes of molecules over macroscopic distances. This indicates the existence of a real thermodynamic phase separation between two disordered liquid phases, a low- (LDL) and a high-density liquid (HDL). The two liquids differ not only in density but also in local order, a feature which has suggested that water thermodynamics are controlled by two order parameters (9).

Recently, extensive studies (43, 44) of the ST2 model have cleared up the field from erroneous results (45), thereby providing definitive evidence of an LL transition in this model. The universality of the LL transition in tetrahedral network fluids has been discussed in studies based on primitive models of patchy colloidal particles (46). It was shown that an LL transition is a generic feature in this class of particles (47) and that a simple extension of the ST2 model for water displays an LLCP that progressively moves to a temperature where the liquid is more stable than ice I_h (44). Finally, we stress that the singularity-free scenario is equivalent to an LLCP scenario in which the critical temperature is located at zero T (9, 48).

Support for the LLCP scenario in water, in addition to the numerical studies of several water (30, 49–54) and water-like (55) potentials, comes from the work of Holten et al. (56). They presented an equation of state, built under the assumption of the presence of a critical component in the free energy, compatible with all available experimental thermodynamic data. Their extended model estimate for the LLCP locus is 0.057 GPa and 214 K (56). Mean-field free energies based on the idea of a chemical equilibrium between two main water classes, supported by the previously mentioned order parameter analysis of computer simulations data, have also been shown to be compatible with the LLCP hypothesis (29, 30, 54).

From the experimental side, indications of the LLCP can be found in the density dependence of the structure factor $S(q)$ and on the analogies between the $S(q)$ measured at low and high pressure and

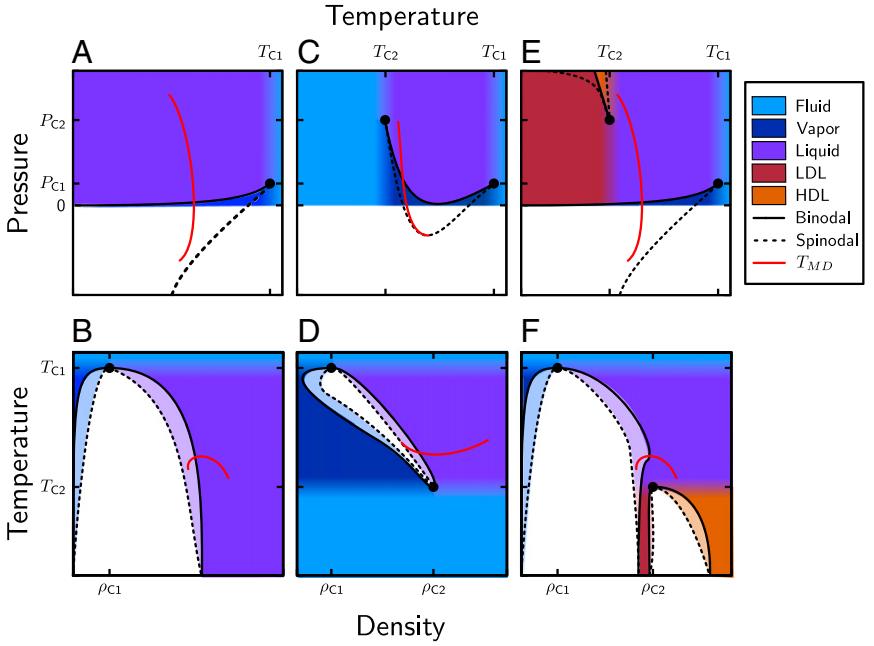

Fig. 1. *P–T* and *T–ρ* phase diagrams of different thermodynamic scenarios for anomalous liquids. Binodals are drawn as solid lines, (mean-field) spinodals as dashed lines, and the T_{MD} line as a red solid line. *A* and *B* show the behavior of a simple system with only a gas–liquid CP (based on ref. 23). *C* and *D* show the behavior of a system with a reentrant spinodal (based on refs. 24 and 25). *E* and *F* show the behavior of a system with a gas–liquid CP and a liquid–liquid (LL) CP (based on the ST2 model in refs. 26 and 27). The light regions in *B*, *D*, and *F* between the binodals and the spinodals are the regions where the corresponding phases are metastable.

the $S(q)$ measured in the low- and high-density amorphous ices (discussed below). Ref. 57 reports the observation of a continuous transformation with increasing P from a low-density form of water with an open, hydrogen-bonded tetrahedral structure to a high-density form of water with nontetrahedral OOO angles and a collapsed second coordination shell. Recent time-resolved optical Kerr effect investigations of the vibrational dynamics and relaxation processes in supercooled bulk water (58) show evidence of the existence of two main local configurations with an increasing weight of the open tetrahedral structure at low T. Consistent interpretations have also been formulated by Sellberg et al. (35) on the basis of X-ray emission and absorption experiments. Strong experimental support in favor of an LL transition has been presented by Mishima and Stanley (59) and Mishima (60). They measured the metastable melting lines of ices III, IV, and V and found discontinuities in the case of ices IV and V and a continuous line in the case of ice III. The discontinuity indicates that the properties of the liquid in equilibrium with the crystal change abruptly, an indirect evidence of the crossing of the line of LL phase transition. The continuous line for ice III indicates that in this case the LL transition line is not crossed. The presence of a possible LLCP is also hinted at by the temperature dependence of the V measured in emulsified water (61), the T and P dependence of the bulk viscosity (62), and experimental studies of water solutions (63–65). In summary, available experimental data suggest the locus of the possible LLCP in the area 214 – 232 K and 0.02 – 0.10 GPa (56, 59, 61).

We note in passing that while the observation of a compressibility maximum at positive P is possibly preempted by crystal nucleation such observation could become accessible at negative P. Very recent experiments in microscopic inclusions of water in quartz building on the seminal work of ref. 66 suggest that this is indeed the case (67, 68).

Amorphous Ice

Polyamorphism. We now turn our attention to the arrested disordered states of water observed below the no-man's land. One of the most intriguing findings in the physics of amorphous water is its polyamorphism, sometimes also called amorphous polymorphism. The term polymorphism indicates the existence of several distinct crystalline phases for the same component. In case of water, 17 ice polymorphs are known to date (69). Adding the term amorphous, however, complicates our affairs. In principle, polyamorphism should indicate the existence of several distinct amorphous phases for the same component. This, however, brings the issue whether or not there are distinct "amorphous phases." Amorphous solids are out-of-equilibrium systems and their properties depend strongly on preparation history. Their properties also change with time and this relaxation proceeds at different rate at different T and P. Consequently, the same phase may appear as a distinct one depending on the state of relaxation. At a certain T, the structural relaxation may either be immeasurably slow, take place on experimentally accessible time scales, or be interrupted by crystallization. If it takes place on accessible time scales and crystallization is slower than observation time the amorphous material passes through numerous relaxation states and ultimately reaches a fully relaxed state. In this metastable equilibrium there is still excess enthalpy and entropy compared with the stable crystalline phase. Thus, a very important measure to judge whether or not amorphous materials may be called "phases" rather than "states" is the separation of time scales between structural relaxation and crystallization.

Taking these considerations into account, we operationally define polyamorphism as the existence of more than one amorphous phase in metastable equilibrium (i.e., nonaging and noncrystallizing). Different amorphous phases have to differ in terms of their properties. Furthermore, just like in the case of distinct crystalline phases, phase boundaries to stable or metastable phases have to exist. We note that phase boundaries between phases with the same symmetry can end in a CP. The usually different symmetry of coexisting crystal phases is indeed the reason why crystal–crystal coexistence lines do not end in a CP. A CP can, however, be the end point of an amorphous–amorphous coexistence line since amorphous phases are isotropic.

Preparation Routes. In the case of water we operationally discriminate three amorphous ices according to their respective density: low- (LDA), high- (HDA), and very-high-density amorphous ice (VHDA). Fig. 2 provides a schematic representation of common paths experimentally used to prepare samples of the three types.

Three paths lead to LDA. Two of these are condensation of gaseous water without crystallization (70) and cooling of the liquid without crystallization. The latter procedure, called vitrification, is the standard procedure of producing a glass. Water, however, is a bad glass former, crystallizing very easily. Thus, hyperquenching at $> 10^6$ K s^{-1} is required to avoid detectable crystallization (71). A third path is via transformation of HDA (e.g., by heating or decompressing HDA) (17, 72). After proper annealing all three routes lead to samples with the same density, structure, and calorimetric behavior, such that all of them are often considered to be the same glass, namely LDA (8). Also for HDA several distinct preparation routes are possible, including quenching of pressurized emulsions of pure water (73) (here cooling rates of 10^3 K min^{-1} are sufficient to avoid crystallization) and pressurizing hexagonal ice at 77 K beyond the low T metastable extension of the liquid–ice coexistence (16). Nowadays, this material is referred to as unannealed HDA (uHDA) to stress its unrelaxed character, whereas its relaxed variant is called expanded HDA (eHDA) (72, 74). HDA can also be prepared from the other two amorphous ices, namely by compressing LDA or by decompressing VHDA (Fig. 2*C*). VHDA can be prepared by pressurizing hexagonal ice at temperatures between about 130 and 150 K (8) or by heating either ice I_h (75) or HDA at high P (76).

Structural Properties. In LDA each water molecule is surrounded by four next neighbors (77), a pattern consistent with ice I_h (78). This indicates LDA is a representation of a fully bonded ideal random tetrahedral network. The vibrational character of LDA is further reminiscent of the one of highly ordered substances, missing the excess density of states characteristic of most other glasses (6). In this respect LDA comes close to the experimental realization of an ideal glass state (6). HDA is characterized by a structure that significantly differs from LDA. At ambient P each molecule has four hydrogen partners on average, but a fifth molecule has moved toward the first shell due to a contraction of the second shell (77). This contraction is even more extreme at 2 GPa where the total coordination number goes up to roughly nine (79). Please note that structurally uHDA and eHDA are very similar. They, however, differ in that they have lots (uHDA) or almost no (eHDA) nanocrystalline domains embedded in the amorphous matrix (80). In the VHDA structure at ambient P even two molecules from the second shell are pushed toward the first shell (81). Hence, the structures of HDA and VHDA significantly differ at ambient P and low T. At high pressures, however, the structural differences between VHDA and HDA become less pronounced, because VHDA is much less compressible than HDA. Klotz et al. (79) have argued that the structure of HDA near 0.7 GPa resembles the structure of VHDA at ambient P.

We note that the cross-over from the four linear HBs in LDA to the distorted HBs where one (HDA) or two (VHDA) interstitial molecules are found between the first and second coordination shell resembles the pressure dependence of the HB pattern in the liquid state.

Amorphous–Amorphous Transitions. The possibility to associate the LDA and HDA structures to the two distinct liquids predicted by the LLCP scenario has prompted a significant experimental effort in the study of amorphous ices, specifically on the stability of and the

relations among the different disordered solid forms. It becomes indeed very relevant to assess if the different high-density forms are members of the same family and if the high- and low-density forms are thermodynamically distinct phases (i.e., whether the glasses are proxies of the two thermodynamically distinct liquids). When tackling those questions, the above-named difficulties due to the peculiarities of amorphous solids arise. For HDA a strong history dependence was reported for the temperature of transformation to LDA at ambient P (82–84) and for T_x at higher P (80). All this makes it particularly important to carefully define the preparation routes when comparing different experiments. For the properly relaxed amorphous state the transformation temperatures reach a limiting value.

HDA can be transformed to LDA by heating at low P. This transformation is accompanied by a $\approx$25% change in density occurring in a jump-like fashion. When first observed, this transformation immediately prompted an interpretation as a first-order transition (17), despite the out-of-equilibrium nature of the entire process. This isobaric transition is irreversible. If, however, an isothermal path at sufficiently high T is followed one can switch back and forth between HDA and LDA (Fig. 2*C*). The transitions on compression of LDA or on decompression of HDA are very sharp and they appear at different P, that is, there is hysteresis (18). This hysteresis can be traced up to the crystallization at T_x (18) and it corroborates the first-order-like nature of the transition. Further evidence for a discontinuous nature of the LDA⇄ HDA transitions was provided by other methods (83, 85). Earlier scattering experiments claiming the possibility of a continuous transition from HDA to LDA (86) can presumably be explained by structural relaxation of HDA preceding the first-order-like transition. Gromnitskaya et al. (87) showed that for well-relaxed samples the initial relaxation stage is absent, simplifying the nature of the transition (88). In our opinion, the experimental evidence, therefore, clearly speaks in favor of LDA and HDA being two distinct amorphous phases, converting through a first-order-like transition. Being a solid–solid transition it is likely influenced by mechanical stress, which should disappear for the HDL⇄LDL transition (89).

While for LDA and HDA experiments show a hysteresis, enabling us to approximately map the binodal, this has so far not been achieved for HDA and VHDA. A binodal between HDA and VHDA, if it exists, is very hard to trace. At low T the observation of the transformation is impeded due to slow kinetics and at higher T due to the small density difference between HDA and VHDA. Despite the difficulty, a relatively sharp density change corresponding to the HDA→VHDA transformation was observed at 125 K (90, 91). This is accompanied by a sudden change of compressibility (92), Raman spectra (92), and relaxation dynamics (93). However, also in this case sample history plays an important role: The sharpness of the density jump was found to decrease with compression rate (90) or to disappear both at lower T (90) and when starting from annealed samples (91). Furthermore, it has been argued that the compressibility and Raman spectra change smoothly (94). The VHDA→HDA transition can also be observed at $T \geq 125$ K but is kinetically hindered at lower T (72, 95). Even though the evidence is ambiguous, we favor the interpretation of a continuous nature of the HDA⇄VHDA transitions at 125 K. Similar conclusions were drawn from isobaric experiments (93, 96, 97). Given the same symmetry of HDA and VHDA, a low-lying CP could exist, possibly located around 0.8 GPa. In any case, confirming or refuting this hypothesis needs future work. Despite these open questions it is fair to state that HDA and VHDA behave as distinct materials if studied at low T. We further note that in aqueous LiCl solution the HDA⇄ VHDA transition fulfills all criteria of a first-order transition (98). In other studies of salty HDA, however, this first-order transition was not found (99, 100).

Phase Diagram of Noncrystalline Water. To provide some guidance Fig. 3 summarizes the P–T behavior of LDA, HDA, and VHDA. We focus specifically on their domain of existence, that is, the P–T window where these glasses can be observed, bounded by the temperatures of crystallization T_x and polyamorphic transition. In this context we also review the calorimetric glass-to-liquid transition as characterized by its onset temperature T_g.

LDA (Fig. 3*A*) exists at relative low P and it crosses over to HDA at higher P. Calorimetric data show the glass transition onset around 136 K at ambient P (101), followed by crystallization. This leaves a small T window where an ultraviscous liquid could exist on the low- T side of the no-man's land. Numerical results suggest that T_g(LDA) should decrease with increasing pressure (103). As a result, the window in which LDL can be studied should widen on increasing P.

HDA (Fig. 3*B*) converts to VHDA when heated at high P and hence its calorimetric T_g and T_x can only be properly characterized at low P. At ambient P HDA can be heated high enough before the conversion to LDA (or LDL), such that a calorimetric glass transition onset around 116 K can be observed (101). This is in fact only the case for eHDA, but not for uHDA. For HDA noncalorimetric experiments suggest that T_g(HDA) increases significantly with pressure (107). Since T_x increases at a similar rate, the T window where HDL could be accessible to experiments remains approximately at the same size upon pressure variation.

VHDA (Fig. 3*C*) converts slowly to HDA at low pressure and hence its calorimetric T_g and T_x can only be properly characterized at high P. On heating at high P, calorimetry data show the onset of a glass transition around 140 K (102). On further heating VHDA crystallizes

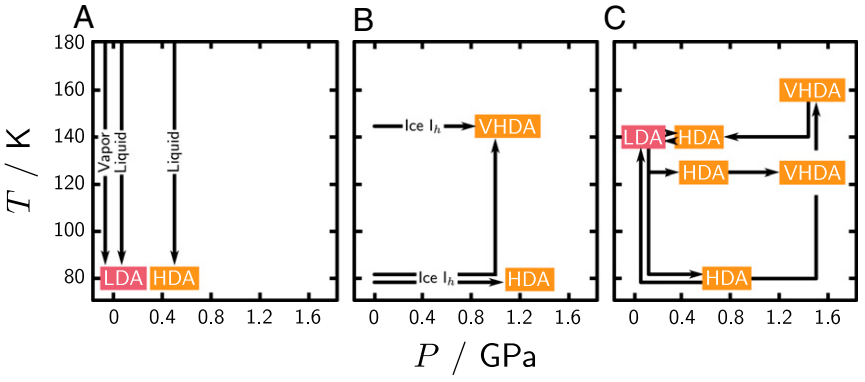

Fig. 2. Preparation routes of amorphous ices in the laboratory. *A* shows paths starting from vapor or liquid water, *B* shows paths starting from hexagonal ice (ice I_h), and *C* shows paths in which an amorphous form is prepared starting from a distinct amorphous ice. Horizontal arrows indicate isothermal compression/decompression paths, and vertical arrows indicate isobaric cooling/heating paths.

to nearly pure ice XII (108). Noncalorimetric experiments suggest (93, 105) that T_g(VHDA) is approximately constant with increased pressure. Since T_x increases the window for a possible observation of the metastable liquid increases with pressure.

Relations Between Glasses and Supercooled Water. The abrupt transition between HDA and LDA on heating at low P or decompressing at sufficiently high T is clearly consistent with the possibility that such a transition is the out-of-equilibrium echo of a true thermodynamic coexistence curve between two (arrested) liquids of different density. The existence of more than one glass of water does resonate with the existence of more than one liquid water form (41). One important precondition for the existence of two distinct liquids is that their relaxation times need to be clearly shorter than their transformation times. It was shown very recently that indeed the dielectric relaxation times in HDA are about three orders of magnitude shorter than the polyamorphic transformation, and similarly the relaxation times in LDA are about three orders of magnitude shorter than crystallization times (109).

The observation of a calorimetric glass transition temperature for HDA (the so-called second glass transition) clearly distinct from the one of LDA has been interpreted as evidence that water has two distinct phases above its glass transition temperatures (101). These phases could possibly be identified as the two distinct ultraviscous liquids, LDL and HDL. This is strong evidence for two distinct metastable liquid forms, one metastable only with respect to crystallization [associated to the T_g(LDA)] and the other metastable both with respect to crystallization and with respect to the low-density liquid form [associated with the T_g(eHDA)]. Evidence in favor of two liquid phases has also been presented in ref. 83. During the experiment, eHDA is decompressed at $T = 140$ K down to 70 MPa. On this path, the sample first crosses the glass transition line where HDA turns into ultraviscous HDL. Then, it crosses the transformation line from HDL to LDL (Fig. 3*B*). Immediate quenching to 77 K at the transformation point freezes the sample. Subsequent visual examination and X-ray diffraction experiments at ambient P show that the sample presents spatially separated regions of LDA and HDA, suggesting that the conversion from HDL to LDL has been interrupted by the quench (83). Very recent ambient pressure static and dynamic X-ray experiments reveal a diffusive collective relaxation process in both LDA and HDA above the glass transition temperature (88). This suggests an ultraviscous liquid nature for LDL and HDL. If this is indeed the case, then the bulk, first-order HDL → LDL transition just below T_x at 70 MPa was experimentally observed in ref. 83.

We stress, however, that even though the interpretation of the previously presented calorimetric data in terms of a glass-to-liquid transition is corroborated by several studies (93, 104–106, 110, 111) the identification of the calorimetric glass transition with the onset of a liquid phase is still debated. Some researchers believe the heat capacity increase to indicate the unfreezing of orientational (as opposed to translational) motion (112, 113). Alternatively, it has been argued that the rise in C_P is a sub-T_g effect (114)—a hypothesis which did not withstand careful scrutiny for LDA (115) and was taken back (116). However, it was revived and is now debated for the case of HDA (117–119). Also, an order–disorder transition (120) or the presence of impurities (121) were quoted as a source of the heat capacity increase, but none of these explanations is able to explain the full phenomenology, for example the rate-dependent shifts of the calorimetric T_g onset. Although the scientific debate on the proper interpretation is ongoing, we do not see any stringent piece of evidence that rules out the interpretation of a transition from glassy solids toward ultraviscous liquids.

Perspectives and Conclusions

In our opinion, three key controversial questions will drive future research on supercooled and glassy water: (*i*) the existence or absence of an LLCP in supercooled water, (*ii*) the number of different amorphous forms of water, and (*iii*) the nature of their glass transition(s).

Concerning *i*, we foresee strong effort in the direction of shrinking the no-man's land from both high and low temperatures, in an attempt to enlarge the accessible window. Most likely the field will see some advance through the application of temperature jump experiments, coupled with ultrafast probing techniques. This will allow measurements of bulk properties in the time interval between (metastable) equilibration and crystallization. One instrumentally highly demanding avenue would be to couple the hyperquenching technique with ultrafast X-ray or laser techniques so that a water droplet can be probed in the microsecond time scale, while it cools from room temperature to 77 K. The detection of extrema in the response functions, especially in the isothermal compressibility, would be highly rewarding, since it could signal the crossing of the Widom line. Large effort will possibly be devoted to fast-quench experiments under high P, to probe the region where the LLCP and the associated HDL–LDL spinodal are expected. The T jump can either be a heating pulse on amorphous ice

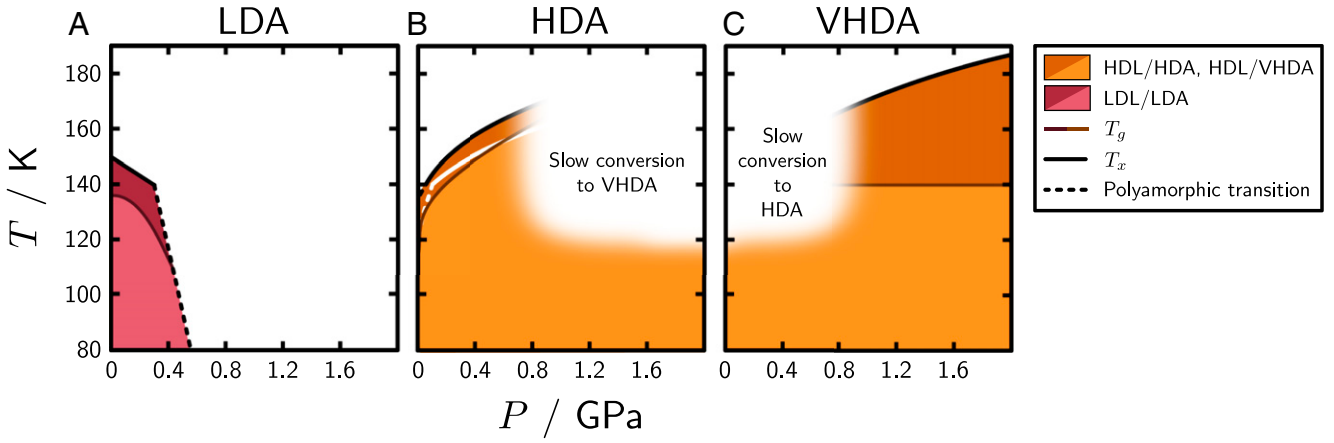

Fig. 3. ***P–T*** **regions of existence of LDA (*A*), HDA (*B*), and VHDA (*C*) including the temperatures of crystallization (T_x) and polyamorphic transition as well as the temperature of the glass-to-liquid transition (T_g). The T_x and polyamorphic transition lines are based on available experimental data quoted in the text. The T_g lines are based on the known calorimetric data (101, 102) in combination with the expected pressure dependence based on numerical (103) and noncalorimetric results (93, 104–106). Note the difference in T_x and in the polyamorphic transition temperature of eHDA (black lines in *B*) and uHDA (white lines in *B*).**

or a cooling pulse on pressurized stable water. For the heating pulses the improved annealing procedures to produce more stable HDA developed over the last few years will be instrumental to access the ultraviscous (metastable) liquid state in between the glass transition and the crystallization temperature. We also expect efforts in the direction of performing this type of sophisticated studies at negative pressures.

On the theoretical side we cannot avoid mentioning it is quite unsatisfactory that rather similar water models apparently predict different behaviors in supercooled states. While it has been claimed that several of them do show an LLCP, it is fair to state that up to today crystal-clear evidence of an LL transition has only been provided for the ST2 water potential. Recent methods devoted to study ST2 water (43) will surely be applied to other models. We do expect that these more sophisticated investigations will clarify under which conditions a model potential shows or does not show (44, 48, 122) an LLCP and how the presence of an LLCP affects the phenomenology of the disordered solid phases (123). We do also expect that future research will focus on the way model parameters affect the thermodynamic scenarios, the barriers to crystallization, and the model glass-forming ability. There is evidence that small variations in the model parameters can convert from an LLCP to a reentrant spinodal scenario as well as from an LLCP to a singularity-free scenario (48, 122). It has also been recently demonstrated (44) that the driving force for crystallization sensitively depends on the bond flexibility and on the softness of the interparticle repulsion (a quantity controlling the ability to interpenetrate). The ultimate goal will definitively be an ab initio quantum-mechanical numerical investigation of supercooled water. Steps in this direction have already been taken. Simulation studies of models with and without an LLCP can also be exploited to assess how the presence of an LLCP affects the phenomenology of the disordered solid phases (123). We note that interesting suggestions on the different thermodynamic scenarios could also come from the investigation of colloidal particles with directional interactions (124–126).

Concerning *ii*, it will be necessary to clarify whether LDA, HDA, and VHDA are the same phase, differing only due their state of relaxation, or whether they are formally separated by thermodynamic transitions. While the majority of results point toward a first-order-like transition between LDA and HDA, much less clear evidence has been presented for an HDA–VHDA transition. The nature of the latter transition can be clarified with present-day technology. Extremely long and slow experiments, requiring a high demand of time and patience, are needed. Furthermore, there is a need to characterize the glass(es) obtained by quenching liquid water at (several) high pressures, from 100 MPa on. The present evidence is limited to Mishima's study at 500 MPa (73). Indeed, while LDA results from ambient pressure hyperquenching, there is no consensus on the materials obtained by quenching at high *P*. Simulation studies seem to suggest that the disordered glass closest to the high-density liquid is the VHDA form (127).

Concerning *iii*, it seems clear that the interpretation of the calorimetric glass transitions of the amorphous ices will continue to receive particular attention. Indeed, under the hypothesis that LDA and HDA are the glass proxies of LDL and HDL evidence of two distinct ultraviscous phases could corroborate the LLCP scenario. Today there is no clear consensus on the origin of the calorimetric signal associated to the low-density form above 136 K (the first glass transition of water) and similarly the high-density form above 116 K (the second glass transition). Clarification of this point is rather relevant: If the calorimetric signal can effectively be associated to a glass-to-liquid transition, then the reported evidence of two distinct T_gs at ambient *P* for LDA and HDA (101) would provide indisputable evidence of two distinct ultraviscous liquid phases. This would offer the possibility to explore metastable LDL and doubly metastable ultraviscous HDL at ambient *P*. We cannot avoid noticing that most of the calorimetric studies have been performed at ambient pressure. Calorimetric studies at higher pressure, in the realm in which HDA and VHDA are more stable, would be most welcome. Such instruments, not commercially available, would be very valuable since it is expected [based on volumetric studies (93, 106)] that also under high *P* an ultraviscous liquid state should exist.

To resolve the conflict on the two opposite interpretations of the calorimetric glass transition (orientational glass versus ultraviscous liquid) novel experiments and novel concepts will be required. This could encompass diffusion studies on tracer molecules as well as mechanical probing of the liquid, for example rheological studies on the sample at 140 K, just after the glass transition and just before its crystallization. Such studies, or studies based on the experimental methods recently exploited to quantify diffusion in ultraviscous water (128, 129), will be most helpful in interpreting the increase in C_P observed both for HDA and LDA at their two distinct T_gs. The same experiments speak in favor of ultraviscous liquid nature, at least for LDA above its T_g (128, 129).

Surely new input from the experimental and theoretical side is highly needed to clear the haze and to come closer to the ultimate goal of understanding water. Based on previous history, it is highly likely that diametric viewpoints will persist and, by competing, drive the field forward.

Acknowledgments

T.L. and F.S. thank all students and collaborators with whom they have been studying this fascinating topic. T.L. thanks in particular R. Böhmer (Technical University of Dortmund), D. T. Bowron (ISIS), and N. Giovambattista (City University of New York) for their long-term collaboration on the subject. We also thank L. Rovigatti and J. Russo for helpful comments on the manuscript. This work was supported by Austrian Science Fund Schrödinger Fellowship J3811 N34 (to P.H.H.), START-Preis Y391, and bilateral project I1392 (T.L.), European Research Council Starting Grant SULIWA (to T.L.), the Austrian Academy of Sciences (several DOC projects for coworkers of T.L.), and ETN-COLLDENSE Grant 642774 (to F.S.).

1 Encrenaz T (2008) Water in the solar system. *Annu Rev Astron Astrophys* 46:57–87.
2 El-Maarry MR, et al. (2017) Surface changes on comet 67p/Churyumov-Gerasimenko suggest a more active past. *Science* 355:1392–1395.
3 Jenniskens P, Blake DF (1994) Structural transitions in amorphous water ice and astrophysical implications. *Science* 265:753–756.
4 Öberg KI (2016) Photochemistry and astrochemistry: Photochemical pathways to interstellar complex organic molecules. *Chem Rev* 116:9631–9663.
5 Debenedetti PG (2003) Supercooled and glassy water. *J Phys Condens Matter* 15:R1669–R1726.
6 Angell C (2004) Amorphous water. *Annu Rev Phys Chem* 55:559–583.
7 Loerting T, Giovambattista N (2006) Amorphous ices: Experiments and numerical simulations. *J Phys Condens Matter* 18:R919–R977.
8 Loerting T, et al. (2011) How many amorphous ices are there? *Phys Chem Chem Phys* 13:8783–8794.
9 Tanaka H (2012) Bond orientational order in liquids: Towards a unified description of water-like anomalies, liquid-liquid transition, glass transition, and crystallization. *Eur Phys J E Soft Matter* 35:113.
10 Caupin F (2015) Escaping the no man's land: Recent experiments on metastable liquid water. *J Non-Cryst Solids* 407:441–448.
11 Nilsson A, Pettersson LG (2015) The structural origin of anomalous properties of liquid water. *Nat Commun* 6:8998.
12 Gallo P, et al. (2016) Water: A tale of two liquids. *Chem Rev* 116:7463–7500.
13 Amann-Winkel K, et al. (2016) Colloquium: Water's controversial glass transitions. *Rev Mod Phys* 88:011002.

14 Amann-Winkel K, et al. (2016) X-ray and neutron scattering of water. *Chem Rev* 116:7570–7589.
15 Mishima O, Stanley H (1998) The relationship between liquid, supercooled and glassy water. *Nature* 396:329–335.
16 Mishima O, Calvert LD, Whalley E (1984) 'Melting ice' I at 77 k and 10 kbar: A new method of making amorphous solids. *Nature* 310:393–395.
17 Mishima O, Calvert LD, Whalley E (1985) An apparently first-order transition between two amorphous phases of ice induced by pressure. *Nature* 314:76–78.
18 Mishima O (1994) Reversible first-order transition between two H_2O amorphs at ∼0.2 GPa and ∼135 K. *J Chem Phys* 100:5910–5912.
19 Finney J (2015) *Water: A Very Short Introduction* (Oxford Univ Press, Oxford).
20 Bianchi E, Largo J, Tartaglia P, Zaccarelli E, Sciortino F (2006) Phase diagram of patchy colloids: Towards empty liquids. *Phys Rev Lett* 97:168301.
21 Stanley HE, Teixeira J (1980) Interpretation of the unusual behavior of H_2O and D_2O at low temperatures: Tests of a percolation model. *J Chem Phys* 73:3404–3422.
22 Sciortino F, Geiger A, Stanley HE (1991) Effect of defects on molecular mobility in liquid water. *Nature* 354:218–221.
23 Sastry S, Debenedetti PG, Sciortino F, Stanley HE (1996) Singularity-free interpretation of the thermodynamics of supercooled water. *Phys Rev E* 53:6144–6154.
24 Sciortino F, Giacometti A, Pastore G (2009) Phase diagram of Janus particles. *Phys Rev Lett* 103:237801.
25 Rovigatti L, Bianco V, Tavares JM, Sciortino F (2017) Communication: Re-entrant limits of stability of the liquid phase and the speedy scenario in colloidal model systems. *J Chem Phys* 146:041103.
26 Poole PH, Saika-Voivod I, Sciortino F (2005) Density minimum and liquid–liquid phase transition. *J Phys: Condens Matter* 17:L431–L437.
27 Smallenburg F, Poole PH, Sciortino F (2015) Phase diagram of the ST2 model of water. *Mol Phys* 113:2791–2798.
28 Stillinger FH, Rahman A (1974) Improved simulation of liquid water by molecular dynamics. *J Chem Phys* 60:1545–1557.
29 Cuthbertson MJ, Poole PH (2011) Mixturelike behavior near a liquid-liquid phase transition in simulations of supercooled water. *Phys Rev Lett* 106:115706.
30 Russo J, Tanaka H (2014) Understanding water's anomalies with locally favoured structures. *Nat Commun* 5:3556.
31 Russo J, Tanaka H (2016) Crystal nucleation as the ordering of multiple order parameters. *J Chem Phys* 145:211801.
32 Hamm P (2016) Markov state model of the two-state behaviour of water. *J Chem Phys* 145:134501.
33 Appignanesi GA, Fris JR, Sciortino F (2009) Evidence of a two-state picture for supercooled water and its connections with glassy dynamics. *Eur Phys J E* 29:305–310.
34 Stillinger FH, Weber TA (1982) Hidden structure in liquids. *Phys Rev A* 25:978–989.
35 Sellberg JA, et al. (2014) Ultrafast x-ray probing of water structure below the homogeneous ice nucleation temperature. *Nature* 510:381–384.
36 Speedy R, Angell C (1976) Isothermal compressibility of supercooled water and evidence for a thermodynamic singularity at −45°C. *J Chem Phys* 65:851–858.
37 Angell C, Shuppert J, Tucker J (1973) Anomalous properties of supercooled water. Heat capacity, expansivity, and proton magnetic resonance chemical shift from 0 to −38°. *J Phys Chem* 77:3092–3099.
38 Speedy RJ (1982) Stability-limit conjecture. An interpretation of the properties of water. *J Phys Chem* 86:982–991.
39 Debenedetti PG (1996) *Metastable Liquids: Concepts and Principles* (Princeton Univ Press, Princeton).
40 Debenedetti PG, D'Antonio MC (1986) On the nature of the tensile instability in metastable liquids and its relationship to density anomalies. *J Chem Phys* 84:3339–3345.
41 Poole PH, Sciortino F, Essmann U, Stanley H (1992) Phase behaviour of metastable water. *Nature* 360:324–328.
42 Xu L, et al. (2005) Relation between the widom line and the dynamic crossover in systems with a liquid–liquid phase transition. *Proc Natl Acad Sci USA* 102:16558–16562.
43 Palmer JC, et al. (2014) Metastable liquid-liquid transition in a molecular model of water. *Nature* 510:385–388.
44 Smallenburg F, Sciortino F (2015) Tuning the liquid-liquid transition by modulating the hydrogen-bond angular flexibility in a model for water. *Phys Rev Lett* 115:015701.
45 Palmer J, et al. (2017) Comment on "The putative liquid-liquid transition is a liquid-solid transition in atomistic models of water" [Parts I and II: J Chem Phys 135, 134503 (2011); J Chem Phys 138, 214504 (2013)]. *J Chem Phys*, in press.
46 Sciortino F (2010) Primitive models of patchy colloidal particles. A review. *Collect Czech Chem C* 75:349–358.
47 Hsu CW, Largo J, Sciortino F, Starr FW (2008) Hierarchies of networked phases induced by multiple liquid–liquid critical points. *Proc Natl Acad Sci USA* 105:13711–13715.
48 Stokely K, Mazza MG, Stanley HE, Franzese G (2010) Effect of hydrogen bond cooperativity on the behavior of water. *Proc Natl Acad Sci USA* 107:1301–1306.
49 Paschek D (2005) How the liquid-liquid transition affects hydrophobic hydration in deeply supercooled water. *Phys Rev Lett* 94:217802.
50 Corradini D, Rovere M, Gallo P (2010) A route to explain water anomalies from results on an aqueous solution of salt. *J Chem Phys* 132:134508.
51 Abascal JL, Vega C (2010) Widom line and the liquid–liquid critical point for the TIP4P/2005 water model. *J Chem Phys* 133:234502.
52 Li Y, Li J, Wang F (2013) Liquid–liquid transition in supercooled water suggested by microsecond simulations. *Proc Natl Acad Sci USA* 110:12209–12212.
53 Ni Y, Skinner J (2016) Evidence for a liquid-liquid critical point in supercooled water within the E3B3 model and a possible interpretation of the kink in the homogeneous nucleation line. *J Chem Phys* 144:214501.
54 Biddle JW, et al. (2017) Two-structure thermodynamics for the TIP4P/2005 model of water covering supercooled and deeply stretched regions. *J Chem Phys* 146:034502.
55 Franzese G, Malescio G, Skibinsky A, Buldyrev S, Stanley H (2001) Generic mechanism for generating a liquid-liquid phase transition. *Nature* 409:692–695.
56 Holten V, Bertrand C, Anisimov M, Sengers J (2012) Thermodynamics of supercooled water. *J Chem Phys* 136:094507.
57 Soper AK, Ricci MA (2000) Structures of high-density and low-density water. *Phys Rev Lett* 84:2881.
58 Taschin A, Bartolini P, Eramo R, Righini R, Torre R (2013) Evidence of two distinct local structures of water from ambient to supercooled conditions. *Nat Commun* 4:2401.
59 Mishima O, Stanley H (1998) Decompression-induced melting of ice IV and the liquid–liquid transition in water. *Nature* 392:164–168.
60 Mishima O (2000) Liquid-liquid critical point in heavy water. *Phys Rev Lett* 85:334–336.
61 Mishima O (2010) Volume of supercooled water under pressure and the liquid-liquid critical point. *J Chem Phys* 133:144503.
62 Singh LP, Issenmann B, Caupin F (2017) Pressure dependence of viscosity in supercooled water and a unified approach for thermodynamic and dynamic anomalies of water. *Proc Natl Acad Sci USA* 114:4312–4317.
63 Suzuki Y, Mishima O (2014) Experimentally proven liquid-liquid critical point of dilute glycerol-water solution at 150 K. *J Chem Phys* 141:094505.
64 Zhao Z, Angell CA (2016) Apparent first-order liquid–liquid transition with pre-transition density anomaly, in water-rich ideal solutions. *Angew Chem Int Ed* 128:2474–2477.
65 Bachler J, et al. (2016) Glass polymorphism in glycerol–water mixtures: II. Experimental studies. *Phys Chem Chem Phys* 18:11058–11068.
66 Green J, Durben D, Wolf G, Angell C (1990) Water and solutions at negative pressure: Raman spectroscopic study to −80 megapascals. *Science* 249:649–652.
67 Pallares G, et al. (2014) Anomalies in bulk supercooled water at negative pressure. *Proc Natl Acad Sci USA* 111:7936–7941.
68 Duška M, Hrubý J, Caupin F, Anisimov MA (2017) Communication: Two-structure thermodynamics unifying all scenarios for water anomalies. arXiv: 1708.04054v1.
69 del Rosso L, Celli M, Ulivi L (2016) New porous water ice metastable at atmospheric pressure obtained by emptying a hydrogen-filled ice. *Nat Commun* 7:13394.
70 Burton E, Oliver WF (1935) X-ray diffraction patterns of ice. *Nature* 135:505–506.
71 Mayer E (1985) New method for vitrifying water and other liquids by rapid cooling of their aerosols. *J Appl Phys* 58:663–667.
72 Winkel K, Elsaesser MS, Mayer E, Loerting T (2008) Water polyamorphism: Reversibility and (dis)continuity. *J Chem Phys* 128:044510.
73 Mishima O, Suzuki Y (2001) Vitrification of emulsified liquid water under pressure. *J Chem Phys* 115:4199–4202.
74 Nelmes RJ, et al. (2006) Annealed high-density amorphous ice under pressure. *Nat Phys* 2:414–418.

75 Handle PH, Loerting T (2015) Temperature-induced amorphisation of hexagonal ice. *Phys Chem Chem Phys* 17:5403–5412.
76 Loerting T, Salzmann C, Kohl I, Mayer E, Hallbrucker A (2001) A second distinct structural 'state' of high-density amorphous ice at 77 K and 1 bar. *Phys Chem Chem Phys* 3:5355–5357.
77 Finney JL, Hallbrucker A, Kohl I, Soper AK, Bowron DT (2002) Structures of high and low density amorphous ice by neutron diffraction. *Phys Rev Lett* 88:225503.
78 Tse JS, et al. (1999) The mechanisms for pressure-induced amorphization of ice Ih. *Nature* 400:647–649.
79 Klotz S, et al. (2002) Structure of high-density amorphous ice under pressure. *Phys Rev Lett* 89:285502.
80 Seidl M, Fayter A, Stern JN, Zifferer G, Loerting T (2015) Shrinking water's no man's land by lifting its low-temperature boundary. *Phys Rev B* 91:144201.
81 Finney JL, et al. (2002) Structure of a new dense amorphous ice. *Phys Rev Lett* 89:205503.
82 Mishima O (1996) Relationship between melting and amorphization of ice. *Nature* 384:546–549.
83 Winkel K, Mayer E, Loerting T (2011) Equilibrated high-density amorphous ice and its first-order transition to the low-density form. *J Phys Chem B* 115:14141–14148.
84 Handle PH, Seidl M, Loerting T (2012) Relaxation time of high-density amorphous ice. *Phys Rev Lett* 108:225901.
85 Klotz S, et al. (2005) Nature of the polyamorphic transition in ice under pressure. *Phys Rev Lett* 94:025506.
86 Tulk CA, et al. (2002) Structural studies of several distinct metastable forms of amorphous ice. *Science* 297:1320–1323.
87 Gromnitskaya EL, Stal'gorova OV, Brazhkin VV, Lyapin AG (2001) Ultrasonic study of the nonequilibrium pressure-temperature diagram of H_2O ice. *Phys Rev B* 64:094205.
88 Perakis F, et al. (2017) Diffusive dynamics during the high-to-low density transition in amorphous ice. *Proc Natl Acad Sci USA* 114:8193–8198.
89 Tanaka H (2000) Thermodynamic anomaly and polyamorphism of water. *Europhys Lett* 50:340–346.
90 Loerting T, et al. (2006) Amorphous ice: Stepwise formation of very-high-density amorphous ice from low-density amorphous ice at 125 K. *Phys Rev Lett* 96:025702.
91 Winkel K (2009) Study of amorphous-amorphous transitions in water (Dr. Hut GmbH, Munich).
92 Salzmann CG, et al. (2006) Isobaric annealing of high-density amorphous ice between 0.3 and 1.9 GPa: *In situ* density values and structural changes. *Phys Chem Chem Phys* 8:386–397.
93 Handle PH, Loerting T (2016) Dynamics anomaly in high-density amorphous ice between 0.7 and 1.1 GPa. *Phys Rev B* 93:064204.
94 Suzuki Y, Tominaga Y (2010) Polarized Raman spectroscopic study of relaxed high density amorphous ices under pressure. *J Chem Phys* 133:164508.
95 Winkel K, et al. (2008) Structural transitions in amorphous H_2O and D_2O: The effect of temperature. *J Phys Condens Matter* 20:494212.
96 Koza MM, et al. (2005) Nature of amorphous polymorphism of water. *Phys Rev Lett* 94:125506.
97 Scheuermann M, Geil B, Winkel K, Fujara F (2006) Deuteron spin lattice relaxation in amorphous ices. *J Chem Phys* 124:224503.
98 Bove LE, Klotz S, Philippe J, Saitta AM (2011) Pressure-induced polyamorphism in salty water. *Phys Rev Lett* 106:125701.
99 Suzuki Y, Mishima O (2009) Differences between pressure-induced densification of LiCl–H_2O glass and polyamorphic transition of H_2O. *J Phys Condens Matter* 21:155105.
100 Ludl AA, et al. (2015) Structural characterization of eutectic aqueous NaCl solutions under variable temperature and pressure conditions. *Phys Chem Chem Phys* 17:14054–14063.
101 Amann-Winkel K, et al. (2013) Water's second glass transition. *Proc Natl Acad Sci USA* 110:17720–17725.
102 Andersson O (2011) Glass-liquid transition of water at high pressure. *Proc Natl Acad Sci USA* 108:11013–11016.
103 Giovambattista N, Loerting T, Lukanov BR, Starr FW (2012) Interplay of the glass transition and the liquid-liquid phase transition in water. *Sci Rep* 2:390.
104 Mishima O (2004) The glass-to-liquid transition of the emulsified high-density amorphous ice made by pressure-induced amorphization. *J Chem Phys* 121:3161–3164.
105 Andersson O, Inaba A (2006) Dielectric properties of high-density amorphous ice under pressure. *Phys Rev B* 74:184201.
106 Seidl M, et al. (2011) Volumetric study consistent with a glass-to-liquid transition in amorphous ices under pressure. *Phys Rev B* 83:100201.
107 Loerting T, et al. (2015) The glass transition in high-density amorphous ice. *J Non-Cryst Solids* 407:423–430.
108 Stern J, Loerting T (2017) Shrinking water's no man's land in the intermediate pressure regime. *Sci Rep* 7:3995.
109 Lemke S, et al. (2017) Relaxation dynamics and transformation kinetics of deeply supercooled water: Temperature, pressure, doping, and proton/deuteron isotope effects. *J Chem Phys* 147:034506.
110 Johari GP (1998) Liquid state of low-density pressure-amorphized ice above its Tg. *J Phys Chem B* 102:4711–4714.
111 Smith R, Kay BD (1999) The existence of supercooled liquid water at 150 K. *Nature* 398:788–791.
112 Fisher M, Devlin JP (1995) Defect activity in amorphous ice from isotopic exchange data: Insight into the glass transition. *J Phys Chem* 99:11584–11590.
113 Shephard JJ, Salzmann CG (2016) Molecular reorientation dynamics govern the glass transitions of the amorphous ices. *J Phys Chem Lett* 7:2281–2285.
114 Yue Y, Angell CA (2004) Clarifying the glass-transition behaviour of water by comparison with hyperquenched inorganic glasses. *Nature* 427:717–720.
115 Kohl I, Bachmann L, Mayer E, Hallbrucker A, Loerting T (2005) Water behaviour: Glass transition in hyperquenched water? *Nature* 435:E1–E2.
116 Angell CA (2007) Glass transition dynamics in water and other tetrahedral liquids: 'order–disorder' transitions versus 'normal' glass transitions. *J Phys Condens Matter* 19:205112.
117 Johari G (2015) Comment on "Water's second glass transition, K. Amann-Winkel, C. Gainaru, P. H. Handle, M. Seidl, H. Nelson, R. Böhmer, and T. Loerting, Proc. Natl. Acad. Sci. (U.S.) 110 (2013) 17720.", and the sub-Tg features of pressure-densified glasses. *Thermochim Acta* 617:208–218.
118 Stern J, et al. (2015) Experimental evidence for two distinct deeply supercooled liquid states of water–response to "comment on 'water's second glass transition"', by GP Johari, Thermochim. Acta (2015). *Thermochim Acta* 617:200–207.
119 Righetti MC, Tombari E, Johari G (2017) Endothermic features on heating of glasses show that the second glass to liquid transition of water was phenomenologically-mistaken. *Thermochim Acta* 647:101–110.
120 Angell C (2008) Insights into phases of liquid water from study of its unusual glass-forming properties. *Science* 319:582–587.
121 McCartney SA, Sadtchenko V (2013) Fast scanning calorimetry studies of the glass transition in doped amorphous solid water: Evidence for the existence of a unique vicinal phase. *J Chem Phys* 138:084501.
122 Poole PH, Sciortino F, Grande T, Stanley HE, Angell CA (1994) Effect of hydrogen bonds on the thermodynamic behavior of liquid water. *Phys Rev Lett* 73:1632–1635.
123 Giovambattista N, Sciortino F, Starr FW, Poole PH (2016) Potential energy landscape of the apparent first-order phase transition between low-density and high-density amorphous ice. *J Chem Phys* 145:224501.
124 Ciarella S, Gang O, Sciortino F (2016) Toward the observation of a liquid-liquid phase transition in patchy origami tetrahedra: A numerical study. *Eur Phys J E* 39:131.
125 Wang Y, et al. (2012) Colloids with valence and specific directional bonding. *Nature* 491:51–55.
126 Smallenburg F, Filion L, Sciortino F (2014) Erasing no-man's land by thermodynamically stabilizing the liquid-liquid transition in tetrahedral particles. *Nat Phys* 10:653–657.
127 Giovambattista N, Stanley HE, Sciortino F (2005) Relation between the high density phase and the very-high density phase of amorphous solid water. *Phys Rev Lett* 94:107803.
128 Hill CR, et al. (2016) Neutron scattering analysis of water's glass transition and micropore collapse in amorphous solid water. *Phys Rev Lett* 116:215501.
129 Xu Y, Petrik NG, Smith RS, Kay BD, Kimmel GA (2016) Growth rate of crystalline ice and the diffusivity of supercooled water from 126 to 262 K. *Proc Natl Acad Sci USA* 113:14921–14925.